From theory to practice

Monitoring mechanical power output during wheelchair field and court sports using inertial measurement units

van Dijk, Marit P.; Hoozemans, Marco J.M.; Berger, Monique A.M.; Veeger, H. E.J.

DOI
10.1016/j.jbiomech.2024.112052

Publication date
2024

Document Version
Final published version

Published in
Journal of Biomechanics

Journal of Biomechanics 166 (2024) 112052

Contents lists available at ScienceDirect

Journal of Biomechanics

journal homepage: www.elsevier.com/locate/jbiomech

From theory to practice: Monitoring mechanical power output during wheelchair field and court sports using inertial measurement units

Marit P. van Dijk [a,1,*], Marco J.M. Hoozemans [b,2], Monique A.M. Berger [c,3], H.E.J. Veeger [a,4]

[a] Department of Biomechanical Engineering, Delft University of Technology, Delft, the Netherlands
[b] Department of Human Movement Sciences, Faculty of Behavioural and Movement Sciences, Vrije Universiteit Amsterdam, Amsterdam, the Netherlands
[c] Centre of Expertise Health Innovation, The Hague University of Applied Sciences, The Hague, the Netherlands

ARTICLE INFO

Keywords:
Mechanical power
Wheelchair sports
Inertial measurement unit
Wheelchair propulsion
Resistance force

ABSTRACT

An important performance determinant in wheelchair sports is the power exchanged between the athlete-wheelchair combination and the environment, in short, mechanical power. Inertial measurement units (IMUs) might be used to estimate the exchanged mechanical power during wheelchair sports practice. However, to validly apply IMUs for mechanical power assessment in wheelchair sports, a well-founded and unambiguous theoretical framework is required that follows the dynamics of manual wheelchair propulsion. Therefore, this research has two goals. First, to present a theoretical framework that supports the use of IMUs to estimate power output via power balance equations. Second, to demonstrate the use of the IMU-based power estimates during wheelchair propulsion based on experimental data. Mechanical power during straight-line wheelchair propulsion on a treadmill was estimated using a wheel mounted IMU and was subsequently compared to optical motion capture data serving as a reference. IMU-based power was calculated from rolling resistance (estimated from drag tests) and change in kinetic energy (estimated using wheelchair velocity and wheelchair acceleration). The results reveal no significant difference between reference power values and the proposed IMU-based power (1.8% mean difference, N.S.). As the estimated rolling resistance shows a 0.9–1.7% underestimation, over time, IMU-based power will be slightly underestimated as well. To conclude, the theoretical framework and the resulting IMU model seems to provide acceptable estimates of mechanical power during straight-line wheelchair propulsion in wheelchair (sports) practice, and it is an important first step towards feasible power estimations in all wheelchair sports situations.

1. Introduction

Wheelchair sports have become increasingly popular over the last decades (Cooper and De Luigi 2014; vanLandewijck and Thompson, 2011). In line with their popularity, monitoring performance in wheelchair sports is becoming more common. Wheelchair sport performance can be monitored by recording time and velocity (Goosey-Tolfrey and Moss, 2005; van der Slikke et al., 2016; de Witte et al., 2018). However, velocity can be biased as a measure of exercise intensity. A large head wind or uneven surface, for example, will generally decrease the velocity, while exercise intensity may be equal. In contrast, the mechanical power exchanged between the athlete-wheelchair combination and the environment, here referred to as mechanical power, is a more objective measure for exercise intensity as not only velocity but also forces are included (van Ingen-Schenau and Cavanagh, 1990). For this reason, mechanical power is often used to provide information on, for instance, training load, physical and physiological capacity, and fatigue, which may support coaches and athletes to reduce injury risks and improve performance (Halson, 2014; Mujika, 2017; Soligard et al., 2016). It should therefore be monitored during wheelchair sports.

In contrast to the well-integrated power meters in professional cycling, obtaining mechanical power during in-field wheelchair sports is

* Corresponding author at: Department of Biomechanical Engineering, Delft University of Technology, Mekelweg 5, 2628CD Delft, The Netherlands.
E-mail address: m.p.vandijk@tudelft.nl (M.P. van Dijk).
[1] ORCID 0000-0002-4900-8084.
[2] ORCID 0000-0001-7358-2601.
[3] ORCID 0000-0002-2014-8817.
[4] ORCID 0000-0003-0292-6520.

https://doi.org/10.1016/j.jbiomech.2024.112052
Accepted 14 March 2024
Available online 17 March 2024

challenging. While bicycles can be equipped with power meters integrated into cranksets or pedals, directly measuring mechanical power in wheelchairs would involve force-instrumented push-rims (de Groot et al., 2014). However, as these systems are expensive, heavy and not sufficiently robust to be used during court sports such as wheelchair basketball or rugby, a non-invasive and inexpensive method to monitor power during wheelchair sports is needed.

One possible method is the use of inertial measurement units (IMUs). IMUs are small wearable sensors that generally contain an accelerometer, gyroscope, and magnetometer, to measure three-dimensional linear acceleration, angular velocity, and the magnetic field, respectively. IMUs can easily be attached to body parts or wheelchair segments and have been used to estimate mechanical power in sports like rowing and cross-country skiing (Gløersen et al., 2018; Uddin et al. 2021; de Vette et al., 2022). As IMUs are used to monitor velocity, acceleration and rotations in wheelchair practice (Bakatchina et al., 2021; Poulet et al., 2022; Rupf et al., 2021; van der Slikke et al., 2015; de Vries et al., 2023), it would be possible to use IMUs for power monitoring as well.

To validly apply IMUs for mechanical power assessment in wheelchair sports, a well-founded and unambiguous theoretical framework is required that follows the dynamics of manual wheelchair propulsion. Although several wheelchair models have been reported previously, they are focused on specific aspects of wheelchair propulsion (e.g. rolling resistance (Cooper, 1990; Sauret et al., 2009; Silva et al., 2017; Teran and Ueda, 2017), athlete/user dynamics (Chenier et al., 2016; Cooper, 1990; Schnorenberg et al., 2014; Veeger et al., 2002; Veeger et al., 1991), or roller systems (Chénier,Bigras,and Aissaoui, 2015; Cooper, 1990) and are, therefore, incomplete or too extensive.

Therefore, the present paper has two goals. First, to present a theoretical framework that supports the use of IMUs to estimate mechanical power via power balance equations. Second, to demonstrate the use of the IMU-based power estimates during wheelchair propulsion based on experimental data.

2. Theoretical framework

2.1. Definition(s) of power

Power is the energy transferred or converted per unit of time and is expressed in Watts. In human locomotion, metabolic energy is converted into muscle power. Subsequently, muscle power enables body segments to overcome internal friction to, eventually, produce external power (e.g., on the push-rims of a wheelchair). However, not all power liberated from metabolic energy is available for locomotion. As energy is required to, for instance, operate the cardio-respiratory system, produce heat, and stabilize the human body, the (metabolic) power input differs from the (mechanical) power output. Power input is essentially equal to the metabolic rate (van Ingen-Schenau and Cavanagh, 1990) and is often measured with respiratory gas analysis systems. Power output is transferred from a – in this case - wheelchair athlete to the environment and it can be approached purely mechanical (see Eq. (1). We therefore refer to power output as ‘mechanical power’. Power can be measured with a wheelchair ergometer, a force-instrumented push-rim, or estimated from kinematic data.

2.2. The power balance for wheelchair propulsion

Following the classic ‘power equations in endurance sports’ of van Ingen-Schenau & Cavanagh (1990), the mechanical power balance of an athlete equals:

$$P_{athlete} = -\sum \boldsymbol{F}_{ext,athlete} * \boldsymbol{v}_{ext,athlete} - \sum \boldsymbol{M}_{ext,athlete} * \boldsymbol{\omega}_{ext,athlete} + \sum \mathrm{d}E_{kin}/\mathrm{dt} \quad (1)$$

$$P_{athlete} = -P_{friction} - P_{gravity} - P_{environmental} + P_{kinetic} \quad (2)$$

In Eq. (1), the effects of gravity are included as an external force (van Ingen-Schenau and Cavanagh, 1990). An alternative way to represent the power equation is given in Eq. (2) (van der Kruk et al., 2018), in which the athlete generates power ($P_{athlete}$) to (partially) overcome power losses due to resistive forces ($P_{friction}$, $P_{gravity}$ and $P_{environmental}$) resulting in a (changing) velocity of the athlete ($P_{kinetic}$). To apply the power balance to a wheelchair athlete, a suitable system must be defined. Two complete yet concise model options are presented below.

2.3. Athlete-wheelchair model

The simplest approach is to consider the athlete-wheelchair combination as a single rigid body. The free body diagram corresponding to this ‘athlete-wheelchair model’ is presented in Fig. 1a. The external forces acting on the athlete-wheelchair model are normal forces ($\boldsymbol{F}_{N,i}$), rolling resistance ($\boldsymbol{F}_{roll,i}$), air resistance ($\boldsymbol{F}_{air,i}$), and gravity ($\boldsymbol{F}_{g,i}$). Throughout this article, internal resistance is considered part of the rolling resistance. No external moments are identified. In the power balance corresponding to the free body diagram, $\boldsymbol{F}_{roll,rear}$ and $\boldsymbol{F}_{roll,front}$ are summarized by $\boldsymbol{F}_{roll,i}$ (see Eq. (3). As normal force is perpendicular to the movement direction of its point of application, it does not produce power and is not included in the power balance. As the rigid bodies are assumed to have no rotations, rotational kinetic energy is not included. Note that the left hand-side of Eq. (3) could be replaced by $\boldsymbol{F}_{propulsion,COM} * \boldsymbol{v}_{COM}$ (see Eq. (4). In all equations, COM refers to the center of mass of the athlete-wheelchair combination (*AW*). In the text, $\mathrm{COM_{AW}}$ is used to avoid confusion.

$$P_{AW} = -\boldsymbol{F}_{roll,COM} * \boldsymbol{v}_{COM} - \boldsymbol{F}_{air,COM} * \boldsymbol{v}_{COM} - \boldsymbol{F}_{g,COM} * \boldsymbol{v}_{COM} + \frac{1}{dt}(0.5 * m_{AW} * \boldsymbol{v}_{COM}{}^2) \quad (3)$$

$$P_{AW} = \boldsymbol{F}_{propulsion,COM} * \boldsymbol{v}_{COM} \quad (4)$$

2.4. Wheelchair model

An alternative approach is to model all forces, moments, and corresponding (angular) velocities, acting on the transportation object, in this case the manual wheelchair (*W*), see Eq. (5). This approach is often used in rowing and kayaking (Doyle et al., 2010; Hogan et al., 2022; Holt et al., 2021; Macdermid and Fink, 2017). For wheelchair propulsion, Chenier et al. (2016) used a similar model to predict instantaneous wheelchair velocity from net force (consisting of average rolling resistance, measured propulsion forces and upper body mass and acceleration). The free body diagram representing this ‘wheelchair model’ is presented in Fig. 1b. With respect to Fig. 1a, four additional terms are introduced: $\boldsymbol{F}_{upperbody,seat}$ and $\boldsymbol{M}_{upperbody,seat}$ representing the force and moment of the upper body on the wheelchair seat induced by upper body movements, $\boldsymbol{M}_{hand,rim}$ representing the moment that the athlete applies on the push-rims around the wheel axes (consisting of both the ‘pure’ moment *and* the tangential force applied by the hands to the push-rim), and $\boldsymbol{\omega}_{wheel}$ representing the wheel angular velocity. As the wheelchair is assumed to have no angular velocity in the sagittal plane, $\boldsymbol{M}_{upperbody,seat}$ produces no power. Consequently, the power produced by the athlete consists of two terms (see Eq. (6).

$$P_W = -\boldsymbol{F}_{roll,W} * \boldsymbol{v}_W - \boldsymbol{F}_{air,W} * \boldsymbol{v}_W - \boldsymbol{F}_{g,W} * \boldsymbol{v}_W + \frac{1}{dt}(0.5 * m_W * \boldsymbol{v}_W{}^2) \quad (5)$$

$$P_W = \boldsymbol{M}_{hand,rim} * \boldsymbol{\omega}_{wheel} + \boldsymbol{F}_{upperbody,seat} * \boldsymbol{v}_W \quad (6)$$

2.5. Model comparisons

Although the instantaneous power graphs of the two models will generally differ from each other, the models are based on the same mechanical principles and can both be used to estimate wheelchair

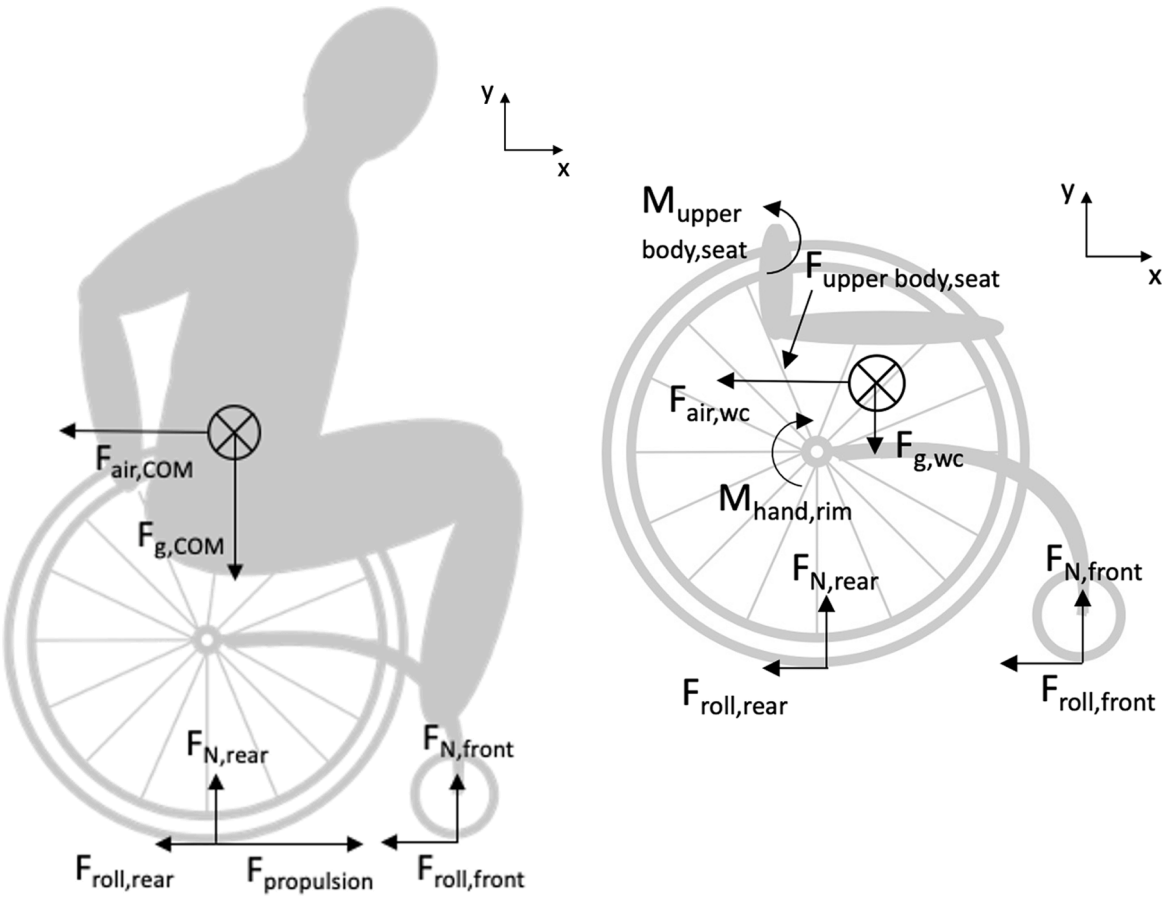

Fig. 1. A-b. Rigid body diagrams with forces acting on the segments. The left figure (a) shows the athlete-wheelchair model. The right figure (b) shows the wheelchair model. Note that the actual direction of the force vectors may be differ from the directions as drawed here. Note also that $\boldsymbol{M}_{hand,rim}$ is drawn at the wheel axes as it represents the moment that the athlete applies on the push-rims around the wheel axes. However, $\boldsymbol{M}_{hand,rim}$ will also apply a moment from the hands on the push-rims around the hand which is described by Van Der Woude et al. (2001) as the 'hand moment'. As this moment is assumed to produce no power, we drawed, $\boldsymbol{M}_{hand,rim}$ around the wheel axes.

athlete power. To understand the differences between the models, let's assume that upper body movements produce no net power on the wheelchair seat (see Appendix A for the situation in which upper body movements *do* produce net mechanical power). In this case, P_{AW} will be non-zero when the hands propel the push-rims, and zero otherwise. Therefore, P_{AW} may be easier to interpret and the instantaneous power graph will be similar to that of a force-instrumented push-rim or ergometer (de Groot et al., 2014); note, however, that P_{AW} will slightly differ from power measured by force-instrumented push rims as force-instrumented push-rims assume that the wheelchair velocity equals the velocity of the COM_{AW} which is not a valid assumption. In the wheelchair model instead, $\boldsymbol{F}_{upperbody,seat}$ is included as a force exerted by the athlete as well. Although $\boldsymbol{F}_{upperbody,seat}$ is zero on average, this force fluctuates within a stroke cycle due to mass displacements of the upper body. Consequently, P_W fluctuates more within a stroke cycle than P_{AW}. However, as P_W consists of mainly wheelchair kinematics (instead of COM_{AW} kinematics, see Eq. (3) and (5), P_W may be easier to approach with IMU data. Because both models have advantages, both were used to underpin and compare with IMU-based power estimates.

3. Power output assessment during wheelchair propulsion with IMU's – From theoretical framework to wheelchair sports practice

In this section, four assumptions are presented to explain how IMU data can be used to approach the different components of the above-mentioned power balance equations.

3.1. Assumptions for power monitoring using IMUs

Assumption 1. (*Mechanical power during wheelchair propulsion can be assessed by monitoring the cycle-average power: cycle-average velocity thus suffices*) *To estimate power output from IMU data, the velocity of the* COM_{AW} (*Eq.* (3) *or the velocity of the wheelchair* (*Eq.* (5), *should be determined. Whereas wheelchair velocity and acceleration can already be measured accurately with an IMU attached to the wheelchair* (van Dijk et al., 2022; van der Slikke et al., 2015), *obtaining the instantaneous velocity and acceleration of the* COM_{AW} *is complex. During propulsion, the* COM_{AW} *moves with respect to the wheelchair due to trunk, head and arm movements* (van Dijk et al., 2021a; van Dijk et al., 2021b). Chenier et al. (2016), *accurately modeled the kinematics of the upper body COM with one IMU on the upper arm. However, they assumed trunk dynamics to be negligible in their spinal cord injury population, which is not reasonable for all wheelchair athletes. Given the differences in movement pattern and heterogeneity of wheelchair athletes, establishing a model that accurately estimates* COM_{AW} *kinematics from IMU data during wheelchair propulsion is complicated and requires multiple body-worn IMUs* (Gløersen et al., 2018; Refai et al., 2020).

However, determining the instantaneous COM_{AW} velocity and acceleration may not be necessary. Many applications in cyclical sports use average power output per push to monitor athletes (Holt et al., 2021; Leo et al., 2022), and this may suffice for wheelchair sports as well. As athletes remain in their wheelchairs during propulsion, one can assume that $\overline{v_{COM}} = \overline{v_{wc}}$ over multiple propulsion cycles, in which $\overline{v_i}$ represents

cycle average velocity.

Assumption 2. (*Air resistance can be neglected during indoor wheelchair field and court sports*) *During wheelchair propulsion, one resistive force acting on the athlete-wheelchair combination is air resistance (see Eq. (3) and (5). To determine air resistance, both the air velocity relative to the wheelchair ($v_{wc/air}$) and the air resistance coefficient ($c_{air,wc}$) should be known (see Eq. (7), Coe, 1979; Forte et al., 2018). As $v_{wc/air}$ varies with wind and wheelchair velocity, and with 'relative' movement direction; and $c_{air,wc}$ depends on air density, streamline and frontal area (de Koning et al., 2005), the information required to calculate air resistance cannot be derived from IMU data. However, in the present paper we focus on indoor wheelchair court sports. As these sports consist of short sprints and lots of braking, the wheelchair velocities are generally below 2.5 m/s (Chénier et al., 2022; van der Slikke et al., 2020). In addition, we assume that air velocity is zero indoors. In these circumstances, the proportion of air resistance is around 5 % of the total resistance force (Barbosa et al., 2014). Therefore, $v_{i/air}$ can be assumed negligible for indoor wheelchair field and court sports.*

$$\boldsymbol{F}_{air,i} = c_{air,i} * \boldsymbol{v}_{i/air} * \left|\boldsymbol{v}_{i/air}\right| \tag{7}$$

Assumption 3. (*The rolling resistance force during wheelchair propulsion can be determined by a deceleration test*) *During indoor wheelchair field and court sports, rolling resistance is the main resistive force (van der Woude et al., 2001). This force can be calculated from the normal forces acting on the rear- and front wheels, and the rolling resistance coefficients of the wheels (see Eq. (8). However, as rolling resistance is influenced by factors such as tire pressure and surface characteristics (Ott and Pearlman, 2021), rolling resistance coefficients may differ for each wheelchair and surface. In addition, the normal force may vary within a propulsion cycle.* Sauret et al. (2013) *assessed the instantaneous normal force acting on the wheelchair wheels and reported that the total normal force varied between 80 and 130 % of the gravitational force. Also, they reported that the normal force at the front wheels fluctuated from 24 to 31 % (minimal values) to 61–83 % (maximal values) of the total load within each push cycle, which might be caused by upper body motions (van Dijk et al., 2021a; van Dijk et al., 2021b). As, in court sports, the front wheels generally have higher rolling resistance coefficients (μ_{front}) compared to the rear wheels (μ_{rear}), this causes intra-cyclical variations in rolling resistance force. To account for these variations, rolling resistance coefficients of each pair of (front or rear) wheels should be determined, and instantaneous normal forces should be known. Unfortunately, normal forces cannot yet be derived from IMU data as this requires information about the COM_{AW} position and vertical acceleration.*

Most studies, however, assume the rolling resistance to be a constant (Chénier et al., 2015; De Groot et al., 2006; Rietveld et al., 2021), that can be determined by a deceleration test (Hoffman et al., 2003; Sauret et al., 2013). During this test, the wheelchair is decelerated from an initial velocity [at which air resistance is assumed negligible, i.e., < 2.5 m/s], at a horizontal surface and while the wheelchair athlete keeps a static posture. Consequently, the resistance force can be calculated from the total mass times the (IMU-based) wheelchair acceleration. During wheelchair propulsion, rolling resistance may thus be estimated by a deceleration test. Note that this test should be repeated once the user, wheelchair (tires) or surface has changed.

$$\boldsymbol{F}_{roll,i} = \boldsymbol{F}_{N,front} * \mu_{front} + \boldsymbol{F}_{N,rear} * \mu_{rear} \tag{8}$$

Assumption 4. (*The role of gravity can be determined from a wheel(chair)-mounted IMU*) *If the surface has a slope, power is transferred to potential energy and should thus be considered in the power balance (see Eq. (3) and (5). The gravitational force ($\boldsymbol{F}_{g,i}$) can be determined from the inclination angle of the wheelchair with respect to the horizontal (θ) and the total mass (according to Eq. (9). With an IMU on the wheelchair frame or wheel and a sensor fusion algorithm that calculates the angle of the wheelchair with respect to the direction of the gravity vector (van Dijk et al., 2021a; van Dijk et al., 2021b), θ can be determined with relative ease. For indoor wheelchair court sports, θ (and thus $\boldsymbol{F}_{g,AW}$) can be considered zero.*

$$\boldsymbol{F}_{g,i} = m_i * 9.81 * \sin(\theta_i) \tag{9}$$

3.2. Implication of assumptions: Simplified power balance for IMU-based estimates

Considering above-mentioned assumptions for wheelchair field and court sports, mean power exchanged between the athlete-wheelchair combination and the environment over multiple stroke cycles can be estimated using one wheel-mounted IMU. Consequently, the power balance for IMU-based power is given in Eq. (10). Here, T is the duration of one complete stroke cycle in seconds. If the assumptions are valid and the wheelchair is unmotorized, the cycle average power output derived from IMU data ($\overline{P_{IMU}}$) should be similar for the athlete-wheelchair model ($\overline{P_{AW}}$) and the wheelchair model ($\overline{P_W}$), see Eq. (11).

$$\overline{P_{IMU}} = (1/T) * \int_0^T \overline{-\boldsymbol{F}_{roll,W} * \boldsymbol{v}_W + \frac{1}{dt}(0.5 * m_{AW} * v_W{}^2)} \tag{10}$$

$$\overline{P_{IMU}} \approx \overline{P_{AW}} \approx \overline{P_W} \tag{11}$$

Monitoring power using IMUs in practice

To demonstrate the use of IMU-based power estimates, power was estimated from IMU data (i.e., $\overline{P_{IMU}}$) during wheelchair propulsion and compared to the power estimated according to the two proposed models (i.e., $\overline{P_{AW}}$ and $\overline{P_W}$) using optical motion capture (MOCAP) data. Although demonstrating this during overground wheelchair propulsion - including curves and turns - would be ideal, the measurement area is limited when using MOCAP and rolling resistance cannot be determined accurately during curves and turns. Therefore, experiments were performed on a large (3.0 x 5.0 m) treadmill. We consider all velocities and accelerations relative to the treadmill belt.

3.3. Methods

This study was approved by the ethical committee of Delft University of Technology (Nr. 1530) and written informed consent was obtained from all participants prior to data collection. Eleven participants (8 female, mean age = 30 ± 9 years, mean body mass = 72 ± 8 kg) without wheelchair experience received a 10-minute training protocol for both overground and treadmill wheelchair propulsion to familiarize with the measurement setup. An IMU (NGIMU, X-io Technologies, Colorado Springs, United States; 100 Hz) was attached to the wheelchair right wheel axle, and marker clusters (Optotrak Certus, Northern Digital, Waterloo, Canada; 100 Hz) were attached to the wheelchair, and participants' body segments (see Fig. 2). The position of anatomical landmarks and wheelchair landmarks relative to the marker clusters was determined. In addition, mass and center of pressure (COP) of the participants + wheelchair was measured on a separate 1.0 x 1.0 m custom-made strain gauge force plate (Kingma et al., 1995). Subsequently, participants propelled an all-court sports wheelchair (13.2 kg) on a large motor-driven treadmill (Bonte, Zwolle, the Netherlands). First, participants propelled at a constant velocity of 1.2 m/s for 90 s, while following a metronome of 25 beats/min (to naturally impose effective strokes and keep a constant power per push). Following this, participants accelerated from 1.2 to 1.7 m/s over a 7-second period imposed by gradually increasing treadmill speed. During the treadmill sessions, three-dimensional kinematics were measured using the IMU and MOCAP system. As performing a deceleration test is not feasible on a treadmill, drag tests were used to obtain $\boldsymbol{F}_{roll}$. After each treadmill session, drag tests were performed at 1.7 m/s while the participants were instructed to sit as still as possible for a period of 30 s in six conditions. The (2x3)

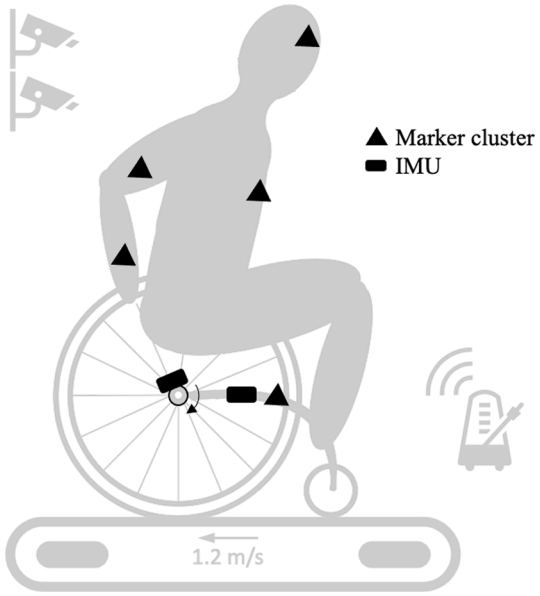

Fig. 2. Overview of the measurement setup. Participants were measured with a MOCAP system with marker clusters (△) on the wheelchair frame, trunk (sternum), head, upper arm and lower arm, and IMUs (□) on the wheel axle and on the center of the wheelchair frame. Both the 3.0 × 5.0 m treadmill and the 1.0 × 1.0 force plate (below the treadmill) are visible in the figure.

conditions consisted of sitting with vertical trunk and sitting bent forward while no mass was added, while 10 kg was added at the footrests and while 10 kg was added on the upper legs. Simultaneously, $\boldsymbol{F}_{roll,inst}$ was measured with a S-beam load cell (Revere Transducers, Lisse, the Netherlands).

3.4. Data analysis

Based on the landmark positions from the MOCAP system, total body length and mass, the upper body segment lengths and COM's were estimated based on the non-linear regression equations as described by Zatsiorsky (2002). Subsequently, upper body segment COM's, m_{AW} and COP of the wheelchair + participant were used to determine the COP of the lower body + wheelchair with respect to the rear-wheel axes. With this information, the horizontal COM_{AW} position (and COM_{AW} velocity vector as its time derivative) relative to the rear-wheel axes could be determined from MOCAP data during the treadmill sessions. COM_{AW} velocity was obtained by summing this 'relative' COM_{AW} velocity to wheelchair velocity. Wheelchair velocity for all models was determined from the wheel-mounted IMU data, wheel circumference, track width and camber angle according to Rupf et al. (2021) and van der Slikke et al. (2015).

Subsequently, instantaneous normal forces were calculated from the horizontal COM_{AW} position relative to the wheels and vertical COM_{AW} acceleration times total mass. Rolling resistance coefficients were numerically solved based on the drag tests with varying load distributions and Eq. (8) (Sauret et al., (2013). The instantaneous normal forces and rolling resistance coefficients were used to determine the instantaneous rolling resistance ($\boldsymbol{F}_{roll,inst}$) according to Eq. (8). $\boldsymbol{F}_{roll,drag}$, determined by a drag test in upright position, was used for $\overline{P_{IMU}}$.

To compare the three different models ($\overline{P_{IMU}}$, $\overline{P_{AW}}$ and $\overline{P_W}$), data were 2nd order low-pass filtered at 6 Hz, after which the instantaneous rolling resistance, dE_{kin} and instantaneous power values were calculated according to Eq. (3), 5 and 10. Subsequently, pushes were identified by the time instance at which the horizontal position of the wrist relative to the wheelchair reaches its maximum. Accordingly, the average values of three consecutive pushes were calculated and again averaged for each participant per condition. The differences between the models were tested statistically using a Wilcoxon signed-rank test (Shapiro-Wilk test revealed no normal distribution) with a significance level of 0.05.

4. Results and discussion of results

The instantaneous power graphs of the three models (see Fig. 3) show that P_{AW} (i.e., athlete-wheelchair model) has a shape similar to the typical shape reported for force-instrumented push-rims (de Groot et al., 2014), while P_W (i.e., wheelchair model) fluctuated within a push cycle due to mass displacements of the upper body. As expected, P_{IMU} fluctuates similarly to P_W as both are based on wheelchair kinematics, with a larger amplitude for P_{IMU} since m_{AW} (Eq. (10) is larger than m_W (Eq. (5). The differences between P_{IMU} and P_{AW} are due to differences between the wheelchair velocity and acceleration (which fluctuates substantially due to upper body motion) and that of the COM_{AW} (which fluctuates much less, see Appendix B) (Table 1).

Cycle average power values of $\overline{P_{IMU}}$ were similar to $\overline{P_{AW}}$ during constant velocity and acceleration. However, $\overline{P_W}$ deviated from $\overline{P_{IMU}}$ and $\overline{P_{AW}}$ during acceleration, because in the wheelchair model, the inertial forces of the upper body (in this case accelerating the upper body mass) is incorporated as athlete force instead of changing kinetic energy. As interpretation of $\overline{P_W}$ may thus be confusing when the velocity is not constant, the wheelchair model is not recommended for estimating power during overground wheelchair propulsion.

However, dE_{kin}/dt *did* differ significantly between $\overline{P_{IMU}}$ and $\overline{P_{AW}}$ (see Table 2). As the first assumption must be true over a longer time duration, dE_{kin}/dt differences between $\overline{P_{IMU}}$ and $\overline{P_{AW}}$ should be similar over time. The difference may be caused by the low number (three) consecutive pushes that have been used for calculation. Due to missing data points in the motion capture data, a larger number of consecutive pushes would load to insufficient data points. Assuming that dE_{kin}/dt differences diminish over several pushes, the accuracy of power output largely depends on the estimated rolling resistance. However, $F_{roll,drag}$ showed an average underestimation of 0.9 % (during acceleration) to 1.7 % (at a constant velocity) of the instantaneous rolling resistance. Moreover, at a constant velocity, this underestimation ranged from −0.9 % to 4.6 % between participants (see Figs. 4 and 5). As this underestimation might be induced by upper body movements, improving the rolling resistance estimate (e.g., by adding an additional IMU on the trunk to correct for trunk-induced effects (Chenier et al., 2016; Poulet et al., 2022; van Dijk et al., 2021a; van Dijk et al., 2021b), might eventually improve power estimates as well.

To summarize, $\overline{P_{IMU}}$ seems an acceptable estimation for power. As it depends largely on the accuracy of the rolling resistance estimate, $\overline{P_{IMU}}$ will be slightly underestimated over several pushes and will improve when rolling resistance estimates improve.

5. Concluding remarks & practical implications

This article proposes a theoretical framework for monitoring mechanical power in wheelchair sports practice. With a well-executed deceleration test and one wheel-mounted IMU, acceptable power estimates can be obtained during wheelchair field and court sports. Based on this feasible approach and the underlying framework, one can elaborate and finetune power estimates for each specific application.

As our results are based on straight-line wheelchair propulsion and rolling resistance usually increases during curves and turns (Chénier et al., 2015; Fallot et al., 2021) one should be aware that the resistance (and thus power) underestimation may be larger when applied in match situations. To accurately monitor power during all match conditions, more knowledge about rolling resistance during turning and trunk inclination is required. External forces due to ball handling and contact with other players will further complicate power estimates. Additionally, accelerations during the experiments were lower than those typically observed during matches. However, as IMUs accurately measure

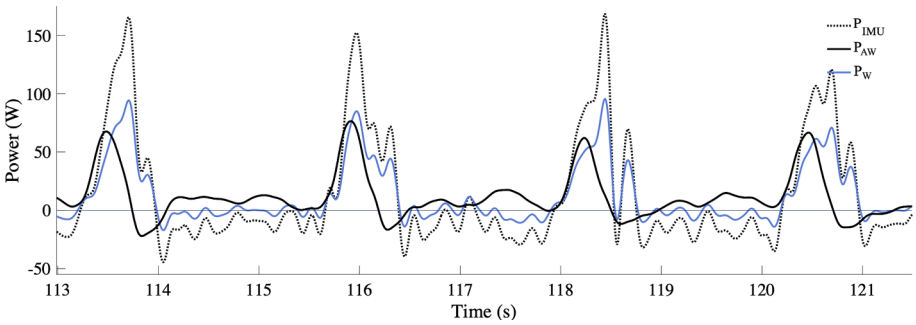

Fig. 3. Typical example of the instantaneous power graph of P_{Aw}(black solid line), P_w (blue solidline) and P_{LMU} (black dotted line) of approximately four pushes at 1.2 m/s.

Table 1
Table of definitions.

i	Point of application
$\boldsymbol{F}_{ext,i}$	External force(s) acting on i
$\boldsymbol{M}_{ext,i}$	External moment(s) acting on i
$\boldsymbol{F}_{roll,i}$	Rolling resistance of i
$\boldsymbol{F}_{air,i}$	Air resistance of i
$\boldsymbol{F}_{g,i}$	Gravity of i
$\boldsymbol{F}_{propulsion}$	Propulsive force
$\boldsymbol{F}_{N,j}$	Normal force acting on wheel j
$\boldsymbol{F}_{source,i}$	Force of source on i
$\boldsymbol{a}_i$	Acceleration of i
$\overline{\boldsymbol{a}_i}$	Cycle-average acceleration of i
$\boldsymbol{\omega}_i$	Angular velocity of i
$\boldsymbol{v}_i$	Linear velocity of i
$\overline{\boldsymbol{v}_i}$	Cycle-average linear velocity of i
$\boldsymbol{v}_{i/ref}$	Velocity of i relative to reference
P_i	Power generated or dissipated by i (i can be a model or a source)
$\overline{P_{model}}$	Cycle average power according to defined model
dE_{kin}/dt	Change in kinetic energy of the chosen system
θ_j	Inclination angle of object j with respect to the horizontal
μ_j	Rolling resistance coefficient of wheel j
$c_{air,j}$	Air resistance coefficient of object j

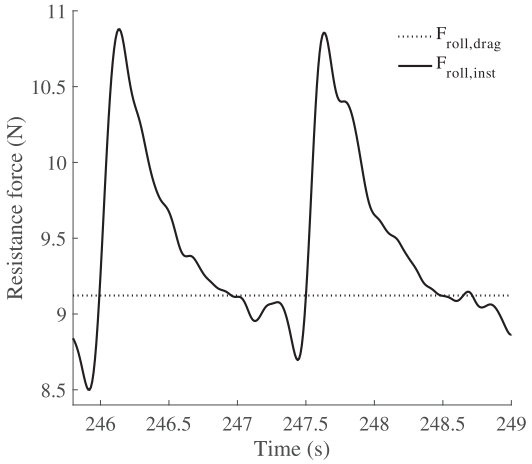

Fig. 4. (left) shows a typical rolling resistance graph during two pushes. The dotted horizontal line shows the resistance force determined from a drag test ($F_{roll,drag}$), and the black curve shows the instantaneous resistance force ($F_{roll,inst}$), in which intra-cyclical changes are taken into account.

Table 2
Mean (S.D.) values and mean (S.D.) differences for power (P), change in kinetic energy ($dE_{kin,i}/dt$) and power loss due to rolling resistance ($P_{roll,i}$, i.e., $\boldsymbol{F}_{roll,i}{}^{*}\boldsymbol{v}_i$) per cycle averaged over three consecutive pushes. The differences are determined by subtracting the variable of the IMU model from the AW model (e.g., P_{AW} - P_{IMU}).

	Absolute values in Watt			Differences		
	IMU model	AW model	W model	in Watt	in % of P_{AW}	*p-value*
Constant velocity						
P	10.7 (1.0)	10.5 (0.9)	10.8 (0.9)	-0.19 (0.25)	−1.8 %	0.11
$dE_{kin,i}/dt$	−0.1 (0.3)	−0.3 (0.3)	−0.2 (0.3)	-0.41 (0.30)*	−3.9 %	0.02
$P_{roll,i}$	10.4	10.6	10.6	0.18 (0.14)*	1.7 %	0.02
Accelerate						
P	16.4 (2.7)	15.7 (2.6)	13.9 (2.1)	-0.71 (0.76)	−4.5 %	0.05
$dE_{kin,i}/dt$	4.1 (1.3)	3.3 (1.3)	1.5 (1.0)	-0.81 (0.73)*	−5.2 %	0.03
$P_{roll,i}$	12.3 (1.6)	12.4 (1.6)	12.4 (1.6)	0.15 (0.06)	0.9 %	0.08

*p-value < 0.05, ** p-value < 0.01.

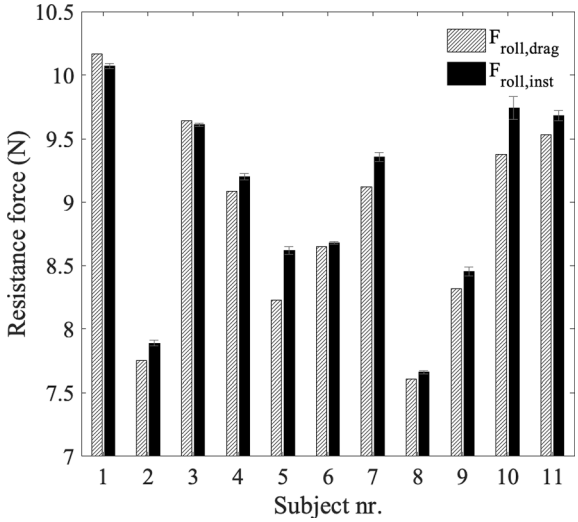

Fig. 5. (right) shows the differences between the resistance values of the drag test ($F_{roll,drag}$) and the average values + standard deviations of the instantaneous resistance force ($F_{roll,inst}$) for each participant. The measurements took place on a treadmill.

wheelchair accelerations, similar accuracies of power estimates are expected at higher acceleration levels. To apply IMU-based power estimates in wheelchair racing, air resistance and gravity should be included as velocities are usually between 5 and 10 m/s (Fuss, 2009; Poulet et al., 2022) and long distance races might contain slopes. For everyday wheelchair use, the power estimates can already be used.

To conclude, we believe that the theoretical framework and the

resulting IMU-model is well suited to estimate mechanical power during straight-line (non-contact) wheelchair propulsion in wheelchair field and court sports. In addition, the framework is an important first step towards feasible power estimates in all wheelchair (sports) situations. As this study is no validation study, the accuracy of $\overline{P_{IMU}}$ may be assessed using force-instrumented push-rims.

CRediT authorship contribution statement

Marit P. van Dijk: Writing – original draft, Visualization, Validation, Software, Resources, Project administration, Methodology, Investigation, Formal analysis, Data curation, Conceptualization. **Marco J.M. Hoozemans:** Writing – review & editing, Supervision, Methodology, Conceptualization. **Monique A.M. Berger:** Writing – review & editing, Methodology, Conceptualization. **H.E.J. Veeger:** Writing – review & editing, Methodology, Conceptualization.

Declaration of competing interest

The authors declare that they have no known competing financial interests or personal relationships that could have appeared to influence the work reported in this paper.

Appendix A

Explanation of the differences between the athlete-wheelchair model and the wheelchair model (and the difference between power estimates based on these models compared to force-instrumented push rims or wheelchair ergometers) when the upper body movements *do* produce net mechanical power.

When the upper body movements *do produce net power.*

When the upper body movements *do* produce net power on the wheelchair seat, for example, when a wheelchair athlete tries to move the wheelchair by using mass displacements only (without touching the rim), this means that $\boldsymbol{M}_{hand,rim}$ from the wheelchair model (see Eq. (5) is zero, while $\boldsymbol{F}_{upperbody,seat}{}^{*}\boldsymbol{v}_{wc}$ will on average be equal to $\boldsymbol{F}_{propulsion,COM}{}^{*}\boldsymbol{v}_{COM}$ of the athlete-wheelchair model (see Eq. (3). However, when using a force-instrumented push-rim, power won't be measured. In addition, in a wheelchair ergometer, $\boldsymbol{F}_{upperbody,seat}$ would not be able to produce power since the wheelchair frame is fixed. When we translate this to normal wheelchair propulsion situations, it becomes clear that any (net) propulsive power produced by $\boldsymbol{F}_{upperbody,seat}$ is neglected by force-instrumented push-rims and wheelchair ergometers. In rowing this phenomenon was also reported and may cause an underestimation of up to 10 % (Hofmijster et al. 2018[1]). As both the wheelchair and athlete-wheelchair model will not have this problem, we assume that comparing the IMU-based power with the power estimates based on these models is a suitable way to demonstrate the usefulness of IMU-based power estimates.

[1] Hofmijster, Mathijs J., Lotte L. Lintmeijer, Peter J. Beek, and A. J. Knoek van Soest. 2018. "Mechanical Power Output in Rowing Should Not Be Determined from Oar Forces and Oar Motion Alone." *Journal of Sports Sciences* 36(18):2147–53.

Appendix B.

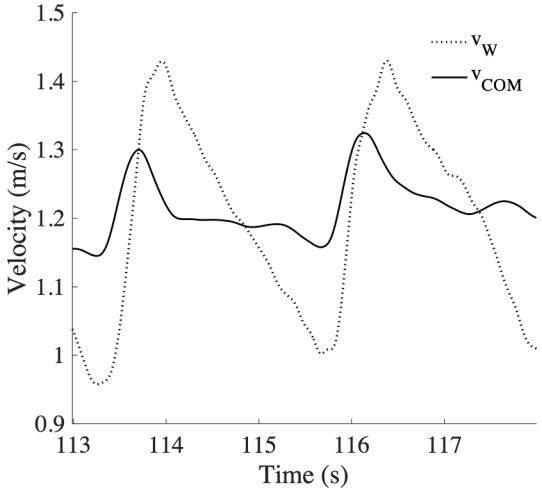

.

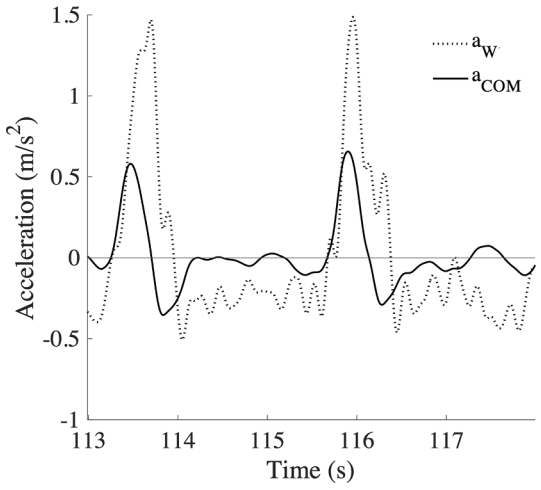

.

Fig 6 and 7. Typical velocity (left) and acceleration (right) graphs of the COM_{AW} (based on motion capture data - solid line) and the wheelchair (based on IMU data - dotted line) during steady state wheelchair propulsion for two pushes. v_W and a_W represent the velocity and acceleration of the wheelchair and v_{COM} and a_{COM} represent the velocity and acceleration of the COM_{AW}. Accelerations are calculated by differentiating velocity over time. The velocity and acceleration of the wheelchair vary more than the velocity and acceleration of the COM_{AW} due to the effect of upper body motion. The negative wheelchair acceleration during recovery can be explained by the upper body movements. Immediately after each push, the upper body accelerates backwards (the small a_W peak right after large a_W peak), and consequently decelerates backwards - until the upper body and wheelchair reach the same velocity when the trunk approaches the back rest - to prepare for the next push. This backward deceleration of the upper body, causes a backward acceleration of the wheelchair (i.e., negative acceleration and decreasing velocity) during recovery as is seen between 114 and 115.5 s.

References

Bakatchina, S., Weissland, T., Astier, M., Pradon, D., Faupin, A., 2021. Performance, Asymmetry and biomechanical Parameters in wheelchair Rugby players. Sports Biomech. 1–14 https://doi.org/10.1080/14763141.2021.1898670.

Barbosa, Tiago, Forte, Pedro, Morais, Jorge E., and Coelho, Eduarda. 2014. "Partial Contribution of Rolling Friction and Drag to Total Resistance of an Elite Wheelchair Athlete." in *Advanced Materials for Sports Technology*. Singapore.

Chénier, F., Bigras, P., Aissaoui, R., 2015. A new dynamic model of the wheelchair propulsion on straight and Curvilinear level-ground paths. Comput. Methods Biomech. Biomed. Eng. 18 (10), 1031–1043. https://doi.org/10.1080/10255842.2013.869318.

Chénier, F., Alberca, I., Gagnon, D.H., Faupin, A., 2022. Impact of sprinting and dribbling on shoulder joint and pushrim kinetics in wheelchair basketball athletes. Front. Rehabilitat. Sci. 3, 863093 https://doi.org/10.3389/fresc.2022.863093.

Chenier, F., Gagnon, D.H., Blouin, M., Aissaoui, R., 2016. A simplified upper-body model to improve the external validity of wheelchair simulators. IEEE/ASME Trans. Mechatron. 21 (3), 1641–11169. https://doi.org/10.1109/TMECH.2016.2527240.

Coe, P. L. 1979. "Aerodynamic Characteristics of Wheelchairs.".

Cooper, R.A., 1990. A systems approach to the modeling of racing wheelchair propulsion. J. Rehabilitat. Res. Dev. 27 (2), 151. https://doi.org/10.1682/JRRD.1990.04.0151.

De Groot, S., Zuidgeest, M., Van Der Woude, L.H.V., 2006. Standardization of measuring power output during wheelchair propulsion on a treadmill. Med. Eng. Phys. 28 (6), 604–612. https://doi.org/10.1016/j.medengphy.2005.09.004.

de Groot, S., Vegter, R., Vuijk, C., Dijk, F., Plaggenmarsch, C., Sloots, M., Stolwijk-Swaeste, J., Woldring, F., Tepper, M., Woude, L., 2014. WHEEL-I: development of a wheelchair propulsion Laboratory for Rehabilitation. J. Rehabil. Med. 46 (6), 493–503. https://doi.org/10.2340/16501977-1812.

de Koning, Jos. J., Carl Foster, Joanne Lampen, Floor Hettinga, and Maarten F. Bobbert. 2005. "Experimental Evaluation of the Power Balance Model of Speed Skating. J. Appl. Physiol. 98(1):227–33. doi: 10.1152/japplphysiol.01095.2003.

de Vette, Vera G., DirkJan (H. E. J.). Veeger, and Marit P. van Dijk. 2022. "Using Wearable Sensors to Estimate Mechanical Power Output in Cyclical Sports Other than Cycling—A Review." *Sensors* 23(1):50. doi: 10.3390/s23010050.

de Vries, W.H.K., van der Slikke, R.M.A., van Dijk, M.P., Arnet, U., 2023. Real-life wheelchair mobility metrics from IMUs. Sensors 23 (16), 7174. https://doi.org/10.3390/s23167174.

de Witte, A.M.H., Hoozemans, M.J.M., Berger, M.A.M., van der Slikke, R.M.A., van der Woude, L.H.V., Veeger, D.H.E.J., 2018. Development, construct validity and test-retest reliability of a field-based wheelchair mobility performance test for wheelchair basketball. J. Sports Sci. 36 (1), 23–32. https://doi.org/10.1080/02640414.2016.1276613.

Doyle, M.M., Lyttle, A., Elliott, B., 2010. Comparison of force-related performance indicators between heavyweight and lightweight rowers. Sports Biomech. 9 (3), 178–192. https://doi.org/10.1080/14763141.2010.511678.

Fallot, C., Bascou, J., Pillet, H., Sauret, C., 2021. Manual wheelchair's turning resistance: swivelling resistance Parameters of front and Rear wheels on different Surfaces. Disabil. Rehabil. Assist. Technol. 16 (3), 324–331. https://doi.org/10.1080/17483107.2019.1675781.

Forte, P., Marinho, D.A., Morais, J.E., Morouço, P.G., Barbosa, T.M., 2018. "The Variations on the aerodynamics of a world-ranked wheelchair sprinter in the key-moments of the stroke cycle: a Numerical simulation analysis" edited by Y.-K jan. PLOS ONE 13 (2), e0193658.

Fuss, F.K., 2009. Influence of mass on the speed of wheelchair racing. Sports Eng. 12 (1), 41–53. https://doi.org/10.1007/s12283-009-0027-2.

Gløersen, Ø., Losnegard, T., Malthe-Sørenssen, A., Dysthe, D.K., Gilgien, M., 2018. Propulsive power in cross-country skiing: application and limitations of a novel Wearable sensor-based method during roller skiing. Front. Physiol. 9, 1631. https://doi.org/10.3389/fphys.2018.01631.

Goosey-Tolfrey, V.L., Moss, A.D., 2005. Wheelchair velocity of tennis players during propulsion with and without the use of racquets. Adapt. Phys. Activ. q. 22 (3), 291–301. https://doi.org/10.1123/apaq.22.3.291.

Halson, S.L., 2014. Monitoring training load to understand fatigue in athletes. Sports Med. 44 (S2), 139–147. https://doi.org/10.1007/s40279-014-0253-z.

Hoffman, M.D., Millet, G.Y., Hoch, A.Z., Candau, R.B., 2003. Assessment of wheelchair drag resistance using a coasting deceleration technique. Am. J. Phys. Med. Rehabilitat. 82 (11), 880–889. https://doi.org/10.1097/01.PHM.0000091980.91666.58.

Hogan, C., Binnie, M.J., Doyle, M., Peeling, P., 2022. Quantifying Sprint kayak training on a Flowing River: exploring the utility of novel power measures and its relationship to measures of relative boat speed. Eur. J. Sport Sci. 22 (11), 1668–1677. https://doi.org/10.1080/17461391.2021.1977393.

Holt, A.C., Hopkins, W.G., Aughey, R.J., Siegel, R., Rouillard, V., Ball, K., 2021. Concurrent validity of power from three on-water rowing instrumentation systems and a Concept2 ergometer. Front. Physiol. 12, 758015 https://doi.org/10.3389/fphys.2021.758015.

Kingma, I., Toussaint, H.M., Commissaris, D.A.C.M., Hoozemans, M.J.M., Ober, M.J., 1995. Optimizing the determination of the body Center of Mass. J. Biomech. 28 (9), 1137–1142. https://doi.org/10.1016/0021-9290(94)00164-Y.

Leo, P., Spragg, J., Podlogar, T., Lawley, J.S., Mujika, I., 2022. Power profiling and the power-duration relationship in cycling: a Narrative review. Eur. J. Appl. Physiol. 122 (2), 301–316. https://doi.org/10.1007/s00421-021-04833-y.

Macdermid, P., Fink, P., 2017. The validation of a paddle power meter for slalom kayaking. Sports Med. Int. Open 01 (02), E50–E57. https://doi.org/10.1055/s-0043-100380.

Mujika, Iñigo. 2017. Quantification of Training and Competition Loads in Endurance Sports: Methods and Applications. Int. J. Sports Physiol. Perform. 12(s2):S2-9-S2-17. doi: 10.1123/ijspp.2016-0403..

Ott, Joseph, Jonathan Pearlman. 2021. "Scoping Review of the Rolling Resistance Testing Methods and Factors That Impact Manual Wheelchairs. J. Rehabilitat. Assist. Technol. Eng. 8:205566832098030. doi: 10.1177/2055668320980300.

Poulet, Y., Brassart, F., Simonetti, E., Pillet, H., Faupin, A., Sauret, C., 2022. Analyzing intra-cycle velocity profile and trunk inclination during wheelchair racing propulsion. Sensors 23 (1), 58. https://doi.org/10.3390/s23010058.

Refai, Mohamed Irfan Mohamed, Bert-Jan F. Van Beijnum, Jaap H. Buurke, and Peter H. Veltink. 2020. "Portable Gait Lab: Instantaneous Centre of Mass Velocity Using Three Inertial Measurement Units." Pp. 1–4 in *2020 IEEE SENSORS*. Rotterdam, Netherlands: IEEE.

Rietveld, T., Mason, B.S., Goosey-Tolfrey, V.L., van der Woude, L.H.V., de Groot, S., Vegter, R.J.K., 2021. Inertial measurement units to estimate drag forces and power output during Standardised wheelchair tennis coast-down and Sprint tests. Sports Biomech. 1–19 https://doi.org/10.1080/14763141.2021.1902555.

Rupf, R., Tsai, M.C., Thomas, S.G., Klimstra, M., 2021. Original article: validity of measuring wheelchair kinematics using one inertial measurement unit during commonly used testing protocols in elite wheelchair court sports. J. Biomech. 127, 110654 https://doi.org/10.1016/j.jbiomech.2021.110654.

Sauret, C., Vaslin, P., Dabonneville, M., Cid, M., 2009. Drag force mechanical power during an actual propulsion cycle on a manual wheelchair. IRBM 30 (1), 3–9. https://doi.org/10.1016/j.irbm.2008.10.002.

Sauret, C., Vaslin, P., Lavaste, F., de Saint, N., Remy, Mariano Cid, 2013. Effects of User's Actions on Rolling Resistance and Wheelchair Stability during Handrim Wheelchair Propulsion in the Field. Medical Engineering and Physics 35 (3), 289–297. https://doi.org/10.1016/j.medengphy.2012.05.001.

Schnorenberg, A.J., Slavens, B.A., Wang, M., Vogel, L.C., Smith, P.A., Harris, G.F., 2014. Biomechanical model for evaluation of pediatric upper extremity joint dynamics during wheelchair mobility. J. Biomech. 47 (1), 269–276. https://doi.org/10.1016/j.jbiomech.2013.11.014.

Silva, L.C.A., Corrêa, F.C., Eckert, J.J., Santiciolli, F.M., Dedini, F.G., 2017. A Lateral Dynamics of a Wheelchair: Identification and Analysis of Tire Parameters. Comput. Method. Biomechan. Biomed. Engineering 20 (3), 332–341. https://doi.org/10.1080/10255842.2016.1233327.

Soligard, T., Schwellnus, M., Alonso, J.-M., Bahr, R., Ben Clarsen, H., Dijkstra, P., Gabbett, T., Gleeson, M., Hägglund, M., Hutchinson, M.R., Rensburg, C.J.V., Khan, K.M., Meeusen, R., Orchard, J.W., Pluim, B.M., Raftery, M., Budgett, R., Engebretsen, L., 2016. How much is too much? (Part 1) International Olympic Committee consensus statement on load in sport and risk of injury. Br. J. Sports Med. 50 (17), 1030–1041. https://doi.org/10.1136/bjsports-2016-096581.

Teran, E., Ueda, J., 2017. Influence of rolling resistance on manual wheelchair dynamics and mechanical efficiency. Int. J. Intelligent Robot. Appl. 1 (1), 55–73. https://doi.org/10.1007/s41315-016-0007-1.

van der Kruk, E., van der Helm, F.C.T., Veeger, H.E.J., Schwab, A.L., 2018. Power in sports: a literature review on the application, assumptions, and terminology of mechanical power in sport Research. J. Biomech. 79, 1–14. https://doi.org/10.1016/j.jbiomech.2018.08.031.

van der Slikke, R.M.A., Berger, M.A.M., Bregman, D.J.J., Lagerberg, A.H., Veeger, H.E.J., 2015. Opportunities for measuring wheelchair kinematics in match settings; reliability of a three inertial sensor configuration. J. Biomech. 48 (12), 3398–3405. https://doi.org/10.1016/j.jbiomech.2015.06.001.

van der Slikke, R.M.A., Berger, M.A.M., Bregman, D.J.J., Veeger, H.E.J., 2016. From big data to rich data: the key features of athlete wheelchair mobility performance. J. Biomech. 49 (14), 3340–4336. https://doi.org/10.1016/j.jbiomech.2016.08.022.

van der Slikke, R.M.A., Berger, M.A.M., Bregman, D.J.J., Veeger, D.H.E.J., 2020. Wearable wheelchair mobility performance measurement in basketball, Rugby, and tennis: lessons for classification and training. Sensors 20 (12), 3518. https://doi.org/10.3390/s20123518.

van der Woude, L.H.V., Veeger, H.E.J., Dallmeijer, A.J., Janssen, T.W.J., Rozendaal, L.A., 2001. Biomechanics and physiology in active manual wheelchair propulsion. Med. Eng. Phys. 23 (10), 713–733. https://doi.org/10.1016/S1350-4533(01)00083-2.

van Dijk, M.P., van der Slikke, R.M.A., Berger, M.A.M., Hoozemans, M.J.M., Veeger, H.E.J., 2021a. Look mummy, no hands! the effect of trunk motion on Forward wheelchair propulsion. 39th ISBS Conference 4.

van Dijk, M.P., Kok, M., Berger, M.A.M., Hoozemans, M.J.M., Veeger, D.H.E.J., 2021b. Machine Learning to improve orientation estimation in sports situations challenging for inertial sensor use. Front. Sport. Active Living 3, 670263. https://doi.org/10.3389/fspor.2021.670263.

van Dijk, M.P., van der Slikke, R.M.A., Rupf, R., Hoozemans, M.J.M., Berger, M.A.M., Veeger, D.H.E.J., 2022. Obtaining wheelchair kinematics with one sensor only? the trade-off between number of inertial sensors and Accuracy for measuring wheelchair mobility performance in sports. J. Biomech. 130, 110879 https://doi.org/10.1016/j.jbiomech.2021.110879.

van Ingen-Schenau, G.J., Cavanagh, P.R., 1990. Power equations in endurance sports. J. Biomech. 23 (9), 865–881.

vanLandewijck, Y.C., Thompson, W.R., 2011. The Paralympic athlete: handbook of sports medicine and science. International Olympic Committee.

Veeger, H.E.J., van der Woude, L.H.V., Rozendal, R.H., 1991. Load on the upper extremity in manual wheelchair propulsion. J. Electromyogr. Kinesiol. 1 (4), 270–280. https://doi.org/10.1016/1050-6411(91)90014-V.

Veeger, H.E.J., Rozendaal, L.A., Van Der Helm, F.C.T., 2002. Load on the shoulder in low intensity wheelchair propulsion. Clin. Biomech. 17 (3), 211–228. https://doi.org/10.1016/S0268-0033(02)00008-6.

Zatsiorsky, Vladimir M. 2002. *Kinetics of Human Motion*. Human Kinetics.